Population genomic analysis provides strong evidence of the past success and future strategies of South China tiger breeding

Chen Wang
Guangzhou Zoo & Guangzhou Wildlife Research Center
Dong-Dong Wu
State Key Laboratory of Genetic Resources and Evolution, Kunming Institute of Zoology, Chinese Academy of Sciences, Kunming, Yunnan, 650223 https://orcid.org/0000-0001-7101-7297
Yao-Hua Yuan
Shanghai Zoo
Meng-Cheng Yao
Kunming Institute of Zoology, Chinese Academy of Sciences
Jian-Lin Han
https://orcid.org/0000-0002-1527-3963
Ya-Jiang Wu
Guangzhou Zoo & Guangzhou Wildlife Research Center
Fen Shan
Guangzhou Zoo & Guangzhou Wildlife Research Center
Wan-Ping Li
Guangzhou Zoo & Guangzhou Wildlife Research Center
Jun-Qiong Zhai
Guangzhou Zoo & Guangzhou Wildlife Research Center
Mian Huang
Guangzhou Zoo & Guangzhou Wildlife Research Center
Shi-Ming Peng
Guangzhou Zoo & Guangzhou Wildlife Research Center
Qin-Hui Cai
Guangzhou Zoo & Guangzhou Wildlife Research Center
Jian-Yi Yu
Shanghai Zoo
Qun-Xiu Liu
Shanghai Zoo
Zhao-Yang Liu
Wangcheng Park

Lin-Xiang Li
Suzhou Shangfangshan Forest Zoo
Ming-Sheng Teng
Chongqing Zoo
Wei Huang
Nanchang Zoo
Jun-Ying Zhou
Chinese Association of Zoological Gardens
Chi Zhang
BGI genomics
Wu Chen (guangzhouchenwu@sina.com)
Guangzhou Zoo
Xiao-Long Tu
Kunming Institute of Zoology, Chinese Academy of Sciences

Article

Keywords:

Posted Date: December 21st, 2021

DOI: https://doi.org/10.21203/rs.3.rs-1157812/v1

Population genomic analysis provides strong evidence of the past success and future strategies of South China tiger breeding

Chen Wang[1,#], Dong-Dong Wu[2,3,4,#], Yao-Hua Yuan[5], Meng-Cheng Yao[2,3,4], Jian-Lin Han[6,7], Ya-Jiang Wu[1], Fen Shan[1], Wan-Ping Li[1], Jun-Qiong Zhai[1], Mian Huang[1], Shi-Ming Peng[1], Qin-Hui Cai[1], Jian-Yi Yu[5], Qun-Xiu Liu[5], Zhao-Yang Liu[8], Lin-Xiang Li[9], Ming-Sheng Teng[10], Wei Huang[11], Jun-Ying Zhou[12], Chi Zhang[13], Wu Chen[1,*], Xiao-Long Tu[2,3,4,*]

1. Guangzhou Zoo & Guangzhou Wildlife Research Center, Guangzhou, 510070, China.
2. State Key Laboratory of Genetic Resources and Evolution, Kunming Institute of Zoology, Chinese Academy of Sciences, Kunming, 650201, China.
3. Kunming Natural History Museum of Zoology, Kunming Institute of Zoology, Chinese Academy of Sciences, Kunming, Yunnan, 650223, China.
4. Kunming College of Life Science, University of the Chinese Academy of Sciences, Kunming, 650204, China.
5. Shanghai Zoo, Shanghai, 200336, China.
6. CAAS-ILRI Joint Laboratory on Livestock and Forage Genetic Resources, Institute of Animal Science, Chinese Academy of Agricultural Sciences (CAAS), Beijing, 100193, China.
7. International Livestock Research Institute (ILRI), Nairobi, 00100, Kenya.
8. Wangcheng Park, Luoyang, 471000, China.
9. Suzhou Shangfangshan Forest Zoo, Suzhou, 215009, China.
10. Chongqing Zoo, Chongqing, 401326, China.
11. Nanchang Zoo, Nanchang, 330025, China.
12. Chinese Association of Zoological Gardens, Beijing, 100037, China.
13. Qinghai Province Key Laboratory of Crop Molecular Breeding, Key Laboratory of Adaptation and Evolution of Plateau Biota, Northwest Institute of Plateau Biology, Chinese Academy of Sciences, Xining, Qinghai, 810008, China.

[#]Authors who made equal contribution to this article.

*Corresponding author. E-mail: guangzhouchenwu@sina.com; tuxiaolong@mail.kiz.ac.cn

Abstract

The South China tigers (*Panthera tigris amoyensis*) are extinct in the wild, but viable populations remain in breeding centers and zoos after 60 years of effective conservation efforts. At present, however, the existing genetic variation of these tigers remains unknown. In this study, we assembled a high-quality chromosome-level genome using long-read sequences and re-sequenced 29 high-depth genomes of the South China tigers. We identified two significantly differentiated genomic ancestries in the extant populations, which also harbored some rare genetic variants introgressed from other subspecies, suggesting limited but essential genetic diversity to sustain the South China tigers. The unique pattern of dual ancestry and the genomic resources generated in our study pay the way for a genomics-informed conservation, following the real-time monitoring and controlled exchange of all reproductive South China tigers.

Introduction

The tiger (*Panthera tigris*) is one of the largest felids and a widely recognized flagship species of wildlife conservation in the world. There are six commonly accepted living tiger subspecies, including the Bengal tiger (*P. t. tigris*), Amur tiger (*P. t. altaica*), South China tiger (*P. t. amoyensis*), Sumatran tiger (*P. t. sumatrae*), Indochinese tiger (*P. t. corbetti*), and Malayan tiger (*P. t. jacksoni*)[1-3]. Among them, the South China tiger is the rarest living subspecies and considered as critically endangered by the IUCN[4]. After their extinction in the wild, considerable efforts have been made to rescue them through captive breeding programs in China.

The Chinese Association of Zoological Gardens commenced a coordinated South China tiger captive breeding and management program in 1994, beginning with 47 tigers of 27 males and 20 females based on the studbook. Detailed pedigree records indicated that all South China tigers are descendants of six individuals, which were kept in the Shanghai Zoo (one male and two females) and the Guiyang Qianling Zoo (one male and two females)[5]. In 2020, there were an estimated 205 South China tigers managed in captivity within China as well as 18 in the Laohu Valley Reserve in South Africa. Signatures of inbreeding such as reduced genetic diversity and low rate of successful breeding have been observed by analyzing the revised studbook of the captive populations of South China tigers[6]. In addition, the hybridization of South China tigers with other tiger subspecies was suggested based on a few mitochondrial and microsatellite markers[7,8]. Considering the positive correction between genetic

heterozygosity and fitness[9,10] as well as the rapid fixation of one allele at individual genetic loci throughout the genomes following the increase in homozygosity and inbreeding load of the individuals in small, managed populations[11,12], it is urgently needed to examine the genomic landscape of existing genetic variation that has driven the past successful rescue of the South China tigers, in reference to large-scale population genomic studies on other tiger subspecies[1,13].

In this study, based on a *de novo* chromosome-level genome assembly and large-scale whole-genome re-sequencing data generated from extant South China tigers, we unexpectedly identified a relatively low genomic inbreeding buffered by two genetically differentiated ancestries in the major captive populations, which also retained some rare genetic variants following the past admixture from other subspecies. These findings not only explained the successful breeding history of the South China tigers in captivity, but also paved the way for the genomics-informed management by applying genome-wide markers to routinely monitor and sustain their critical genetic variation in the future.

Results

De novo genome assembly and whole-genome re-sequencing of the South China tigers

To investigate the genetic variation and evolution of South China tigers (Fig. 1a), we first constructed a high-quality *de novo* assembly of the South China tiger genome

using a combination of high-fidelity short-read sequencing[14], long-read single-molecule real-time sequencing[15], optical mapping[16], and Hi-C[17] technologies. We generated a total of 122.31 Gb (50.96×) of PacBio long reads, 1,011.73 Gb (421.55×) of Illumina paired-end short reads, 440.32 Gb (183.47×) of BioNano optical molecules, and 532.46 Gb (221.86×) of Hi-C data (Supplementary Tables S1 and S2). K-mer[18] analysis revealed its genome size to be 2.47 Gb (Supplementary Figure 1, Supplementary Table S3). After being polished and finally corrected using the Illumina short reads, the PacBio-based initial assembly resulted in a contig N50 at 6.20 Mb. We scaffolded the PacBio contigs using the BioNano optical mapping data. The resulting scaffolds were further clustered into chromosome-scale scaffolds using the Hi-C data (Supplementary Figure 2). Finally, the *de novo* assembly generated 2.44 Gb of genomic sequences with a contig N50 at 6.13 Mb and a scaffold N50 at 150.19 Mb (Fig. 1b, Supplementary Table S4). This novel assembly is the runner-up genome after the one of African lion among all big cats and serves as the best reference genome of tiger species up to today[13,19-22]. The *de novo* assembly contained 19 pseudochromosomes anchored with 2.40 Gb of contigs (99.35%) and 2.42 Gb of scaffolds (99.36%), showing a high collinearity with the reference genome (FelCat9.0) of the domestic cat (*Felis catus*) (Ensembl release 98, accessed in September 2019), except for the E3 chromosome (Supplementary Figure 3, Supplementary Table S5). BUSCO[23] result demonstrated this novel genome to be 95.50% of its completeness (Supplementary Table S6). By integrating the homology- and *de novo*-based predictions, a total of 844.92 Mb (34.98%) of repetitive elements and 20,910

protein-coding genes were annotated (Supplementary Tables S7-S9). In addition, we predicted non-coding RNA genes, including 568 microRNA (miRNA), 6,309 transfer RNA (tRNA), 993 ribosomal RNA (rRNA), and 1,410 small nuclear RNA (snRNA) genes (Supplementary Table S10). Altogether, we produced the first high-quality chromosome-level assembly of the South China tiger genome (Supplementary Figures 4 and 5).

To explore genetic variation lasted in the extant South China tigers, we re-sequenced the whole genomes of 29 individuals collected from several major zoos in China. A domestic cat was also re-sequenced and used as an outgroup (Fig. 1c). We generated around 1,200 Gb of whole-genome sequencing data with an average coverage depth of 15.63×. We combined our data with 40 previously published genomes of other five tiger subspecies (10.38-29.59× coverage depths) (Supplementary Figures 6 and 7, Supplementary Tables S11-S13). We identified 10.21 million high-quality single nucleotide polymorphisms (SNPs) in 69 tiger and one cat genomes after the stringent quality control and the alignment of all re-sequencing data against our novel South China tiger genome (Supplementary Figure 8, Supplementary Tables S14 and S15).

Two genomic ancestries sustained the extant South China tigers

To clarify the phylogenetic relationship and genetic background of different tiger subspecies, we performed principal component analysis (PCA) (Supplementary Figures 10 and 11) and a model-based ancestry estimation using ADMIXTURE

133 software to infer their population genetic structure (Figure 2b, Supplementary Figure
134 9b). We found that all tiger subspecies were clearly diverged from each other, despite
135 potential gene flow among some of them, while the South China tigers were further
136 differentiated into two subgroups at the best K = 5. We further reconstructed
137 neighbor-joining (NJ) trees based on pairwise genetic distances with domestic cat as an
138 outgroup, which clearly supported the taxonomic status of six distinct living tiger
139 subspecies[1,3,24,25] (Fig. 2a, Supplementary Figure 9a). The maximum-likelihood tree
140 (Supplementary Figure 12) and identity-by-state analysis (Supplementary Figures
141 13-15) all verified this divergence pattern at subspecies level.
142
143 Based on the phylogenetic tree and the population genetic structure inferred by
144 ADMIXTURE, two clearly differentiated genomic ancestries (subgroups 1 and 2) were
145 identified among the South China tigers (Fig. 2a and 2b), a probable result of recent
146 but long assortative mating, as what was observed in the killer whale ecotypes[26] and
147 highly inbred pigs[27], driving allelic segregation in the two tiger subgroups. The
148 inference by both MSMC2 (Fig. 2c) and δaδi analyses (Supplementary Table S16) for
149 the potential scenario of these two ancestries suggested their initial segregation as early
150 as 3,000 years ago, while the divergence between the South China tiger and its closest
151 counterpart, the Amur tiger, was estimated around 20,000 years ago (Supplementary
152 Figure 16), to be highly similar to a previous study[1]. Thus, these findings confirmed
153 the presence of these two genomic ancestries among major South China tiger
154 populations.

155

156 **Limited gene flow from other tiger subspecies to extant South China tigers**

157 To detect signal of potential genetic introgression from other tiger subspecies into the
158 South China tigers, we applied several population genetic analyses, including the
159 ABBA-BABA test[28,29], *f4*-ratio[30], and TreeMix method[31]. The results clearly indicated
160 that the South China tiger sequenced by Liu et al.[1] displayed the highest admixture
161 signal of hybrid origin from other subspecies (Fig. 2b and 2d). Although genetic
162 admixture occurred among tiger species (Supplementary Figures 17-19,
163 Supplementary Tables S17 and S18), we found a very low level of such introgression
164 (0.13-1.50%) into the South China tiger genomes (Fig. 2d).

165

166 **Pattern of genetic variation among six tiger subspecies**

167 All tiger subspecies have been experiencing severe population bottlenecks due to
168 human hunting and habitat fragmentation. Here, we compared the levels of genetic
169 diversity and population differentiation among these subspecies. It was evident that the
170 Sumatran tigers showed the least genetic diversity in terms of both genome-wide
171 heterozygosity and nucleotide diversity ($\pi = 0.553 \times 10^{-3}$) (Supplementary Figures 20
172 and 21, Supplementary Table S19) but the highest genetic differentiation from other
173 five tiger subspecies (F_{ST} = 0.324-0.459) (Supplementary Table S20), confirming the
174 observations of previous studies[1,13]. Five Amur tigers had significantly higher
175 heterozygosity than the remaining six individuals (Fig. 3a), a clear genetic
176 sub-structuring within this subspecies due most likely to the recent admixture with

177 other subspecies. However, the level of genetic diversity in all South China tiger
178 populations was not as low ($\pi = 0.657 \times 10^{-3}$) (Supplementary Table S19) as what we
179 expected, following their pedigrees recorded in the studbook. Nonetheless, the South
180 China tigers also showed a significant genetic differentiation from other tiger
181 subspecies (F_{ST} = 0.278-0.459) (Supplementary Table S20).
182
183 We determined the relatedness among individuals within each tiger subspecies using
184 allelic identity-by-descent (IBD)[26] and identified their different levels of inbreeding
185 (Fig. 3b, Supplementary Table S21). Further, we calculated individual inbreeding
186 based on whole genome SNPs using the inbreeding coefficients F_H (a measure of the
187 increase in individual SNP homozygosity compared with mean Hardy-Weinberg
188 expected homozygosity) and F_{ROH}[32] (based on runs of homozygosity (ROH) > 100 kb).
189 Both analyses demonstrated the highest level of genome-wide inbreeding in the
190 Sumatran tigers, due probably to their founder event and strong recent bottleneck
191 (Supplementary Figure 22, Supplementary Table S22), while both Amur and South
192 China tigers had higher F_{ROH} values under longer ROH (1-2 Mb and > 2 Mb), an
193 indication of their recent inbreeding/founder events and/or population
194 bottleneck/isolation (Fig. 3c). Although the pedigree-based inbreeding coefficients (F_p)
195 of the South China tigers were calculated as high as 0.1796-0.5048[5], the genomic IBD
196 was validated to be more strongly correlated with both F_H and F_{ROH} than F_p when
197 high-density SNPs are available[33]. The genome-wide SNP-based individual inbreeding
198 estimates from this study are thus recommended for assisting the decision-making of

captive breeding of the South China tigers.

Because of the importance of managing deleterious mutations in conserved genomic elements for species conservation[34], we calculated the proportion of deleterious mutations retained in potential coding regions of the six tiger subspecies and obtained a total of 73,979 SNPs, 0.562% of which carried highly deleterious mutations, most of them to be stop-gain, across all tiger subspecies (Supplementary Table S23). There was no significant difference in high-, moderate-, and low-impact variants among the tiger subspecies (Fig. 4a). The derived allele frequency distribution of high- and moderate-impact mutations in the South China tigers did not display downward shifts compared to low-impact mutations (nearly neutral) (Fig. 4b). Furthermore, the numbers of homozygous sites with high-, moderate-, and low-impact mutations were the lowest in the South China tigers compared with other subspecies (Fig. 4c, Supplementary Table S24). Despite their inbreeding history, we did not observe the accumulation of deleterious mutations or purging of highly deleterious mutations in the South China tiger genomes, to be in a sharp contrast with many endangered mammals experiencing severe bottlenecks and inbreeding[35-37]. This distinct distribution pattern of deleterious mutations may have also facilitated the successful captive breeding and rapid population recovery of the South China tigers.

Discussion

In the present study, we assembled a high-quality chromosome-level genome of the

South China tiger, to provide a reference for further genetic and genomic studies of all tigers. We found very limited genetic admixture from other tiger subspecies, suggesting very little or even no genetic erosion in the South China tigers. This finding contradicts previous opinions that "non-pure" tigers are caused by hybridization[7,8]. However, we have only re-sequenced the whole genomes of 29 South China tigers collected from four core breeding zoos in China, despite there are more than 200 South China tigers today. As such, we shall continue and focus our efforts on collecting and re-sequencing additional whole genomes of most, if not all, reproductive South China tigers, to further fine-map and effectively manage their viable genomic landscapes along with unique genetic variants present among their major populations.

Analysis of the different characteristics of genetic variation showed that, compared with other tigers, the South China tigers harbored a moderate level of genetic diversity, but escaped from the accumulation of harmful mutations in their conserved genomic regions. We identified two genomic ancestries lasted in existing South China tiger populations, as a probable outcome of recent segregation event and/or genetic drift from limited founders being kept and reproduced in isolated zoos. However, we inferred the differentiation time to be about 3,000 years ago. The Chinese Association of Zoological Gardens has been coordinating the South China tiger captive breeding and management program since 1994. All South China tigers are considered as the descendants of one wild-caught tigress from Fujian and five wild-caught tigers from Guizhou between 1958 and 1970[5]. Our results clearly corroborated the existence of

these two lineages. We therefore recommend a genomics-informed management of these two genetic ancestries, to minimize a further loss of the unique and critical genetic variants but a potential increase in the inbreeding load across all South China tiger populations. All the new findings from our present study demonstrate the power and effectiveness of concerted efforts to conserve the South China tigers in the past and shed light into a potentially bright future of these critically endangered cats, to be another case as what is achieved in the conservation of Giant Panda to be off the endangered list of IUCN[4].

Materials and methods

De novo genome sequencing

Blood samples of one male (Tuantuan) and another female (Huanhuan) South China tiger were acquired from Guangzhou Zoo for genome sequencing. All libraries were constructed at BGI (Shenzhen, China). Three short insert libraries (270, 500, and 800 bp) were constructed for Tuantuan and four long mate-paired insert libraries (2, 5, 10, and 20 kb) were constructed for Huanhuan. All libraries were sequenced on the Illumina HiSeq X Ten Platform using 150-bp paired-end reads according to the Illumina protocols, except for the 800-bp library, which was sequenced on the HiSeq2500 System using 125-bp paired-end reads. Genomic DNA from the Tuantuan blood sample was also used to prepare libraries for sequencing on a PacBio RS II sequencer.

Estimation of genome size

We applied 17-mer distribution analysis to estimate the tiger genome size using clean reads from the short-insert libraries. Genome size was calculated using the formula: Genome size = K-mer_num / Peak_depth.

Genome assembly

The PacBio data were *de novo* assembled using WTDBG-1.2.8 (https://github.com/ruanjue/wtdbg-1.2.8) and genomic contigs were polished with the Arrow program (https://www.pacb.com/support/software-downloads/) by aligning SMRT reads, which yielded an assembly (2.43 Gb in length) with N50 size at 6.24 Mb. We also aligned the Illumina X Ten data to the assembly using BWA (v0.7.15)[38] for error correction by Pilon (v1.22)[39] with the parameter '--mindepth 6', which is an integrated tool for comprehensive variant detection and genome assembly improvement. The final assembly generated a total length of 2.42 Gb and N50 length at 6.20 Mb.

Construction of optical genome maps

DNA of sufficient quality was extracted and labelled from the Tuantuan blood cells according to standard BioNano protocols (BioNano Genomics), after which nicking, labeling, repairing, and staining processes were implemented. We digested DNA using a specific single-stranded nicking endonuclease (Nt.BspQI). BioNano Solve (v3.0.1)[40] was used to produce optical maps with single molecules above 100 kb in size and six

287 labels per molecule. The scaffold-level assembly had a N50 length at 31.62 Mb.

288

289 **Hi-C analysis**

290 The Hi-C library was constructed from the blood cells of a male South China tiger
291 (Kangkang) according to the standard procedures of BGI and sequenced using the
292 MGISEQ-2000 Platform. The BioNano-based scaffolds were anchored into a
293 chromosome-scale assembly using a Hi-C proximity-based assembly approach. We
294 aligned the Hi-C reads to scaffolds using bowtie2 (v2.2.5)[41] and interaction maps were
295 generated following HiC-Pro (v2.5.0)[42] pipelines. The uniquely mapped read pairs
296 were used as input for Juicer[43] and 3d-DNA[44] Hi-C analysis and scaffolding pipelines.
297 The resulting Hi-C contact maps were visualized using Juicebox[45], and mis-assemblies
298 and mis-joins were manually corrected based on neighboring interactions. The final
299 chromosome assembly was then generated.

300

301 **Genome annotation**

302 We identified repetitive sequences in the genomes using a combination of homology-
303 and *de novo*-based methods. First, RepeatMasker[46] and RepeatProteinMask[46] were
304 used to search repeat sequences against with Repbase database[47,48]. Second,
305 LTRharvest (GenomeTools v1.5.9)[49] and RepeatModeler
306 (http://www.repeatmasker.org/RepeatModeler/) were used to build a *de novo* repeat
307 library, and then repeats were annotated using RepeatMasker[46] with default parameters.
308 Last, tandem repeats were detected using Tandem Repeats Finder (TRF)[50].

For gene structure prediction, we used homology-based prediction based on the protein sequences from five species (*Felis catus*, *Homo sapiens*, *Mus musculus*, *Panthera pardus*, and *Panthera tigris altaica*) downloaded from the Ensembl database (release 93). These protein sequences were mapped to the South China tiger genome using TBLASTN (E-value cutoff: $1e^{-5}$)[51]. High-scoring segment pairs (HSPs) were concatenated using Solar (v0.9.6)[18]. GeneWise (v2.4.1)[52] was used to define accurate gene models. We then merged and filtered redundancy from different homology results based on the GeneWise score (≥ 0.4). To obtain the final gene set, transposons and single-exon genes without functional annotations were filtered out.

Gene functional annotations were assigned using BLASTP (BLAST+ v2.2.26)[51] against public databases, including the Swiss-Prot (release-2017_09)[53], TrEMBL (release-2017_09)[53], KEGG (v84.0)[54], COG[55], and NCBI nucleotide collection nr/nt (https://www.ncbi.nlm.nih.gov/nucleotide/, v20170924). The motifs and domains in the protein sequences were annotated using InterProScan (v5.16-55.0)[56].

The tRNA genes were predicted using tRNAscan-SE (v1.3.1)[57] with eukaryote parameters. The rRNA fragments were identified by aligning the rRNA template sequences from the Human Rfam database[58] using BLASTN (BLAST+ v2.2.26)[51] (E-value 1e-5). The snRNAs and miRNAs were searched via a two-step method: i.e., aligned with BLAST and then searched with INFERNAL (infernal-1.1.1)[59] against the

Rfam database.

Sampling information and genome re-sequencing. We collected a total of 30 specimens, including 29 South China tigers (*P. t. amoyensis*) from several major zoos in China and a domestic cat (*Felis catus*) from Guangzhou Zoo, China (Supplementary Table S11). Genomic DNA was extracted from whole blood using the DNeasy Blood & Tissue Kit (QIAGEN, Valencia, California, USA) following the manufacturer's protocols. Sequencing libraries were prepared according to the Illumina library preparation pipeline and sequenced using the Illumina Hiseq X Ten platform to generate 150-bp paired-end reads.

Quality control. To ensure reads were reliable and without artificial bias (e.g., low-quality paired reads that result from base-calling duplicates and adapter contamination), we conducted a series of quality control (QC) procedures, as follows:

(1) Removed reads with ≥ 1% unidentified nucleotides (N).

(2) Removed reads with > 40% bases having phred quality < 20.

(3) Removed reads with > 10 nucleotides overlapping the adapter (allowing ≤ 10% mismatches).

Read alignment and variant calling. We used BWA[60] to align the clean reads of each sample against our newly assembled South China tiger genome (settings: mem -t 4 -k 32 –M -R). Alignment files were converted to BAM files using SAMtools (settings:

–bS –t) (v-0.1.19)[61]. In addition, potential PCR duplications were removed using Picard (http://broadinstitute.github.io/picard/). We called SNPs using the HaplotypeCaller approach implemented in the Genome Analysis Toolkit (GATK) package[62]. Filtering criteria were as follows:

(1) SNPs with (QD < 2.0; FS > 60.0; MQ < 40.0; QUAL < 30; DP < 4.0; MQRankSum < –12.5; ReadPosRankSum < –8.0) were filtered.

(2) Multi-nucleotide polymorphisms were ignored.

(3) SNPs within 5 bp of a gap were filtered.

(4) Overall depth (for all individuals) was > 1/3× and < 3×.

(5) Unobserved variant allele constituted < 10%.

A total of 54,067,600 high-quality SNPs were retained for subsequent analyses after filtering. Gene-based SNP annotation was performed using ANNOVAR[63].

Phylogenetic and population genetic analysis. We selected whole-genome SNPs and four-fold-degenerate sites (4D-sites) that represent neutral or near-neutral variants for phylogenetic and population structure analyses. PCA was performed using PLINK (v1.9)[64]. Genetic structure was inferred using ADMIXTURE (v1.3)[65], with implementation of a block-relaxation algorithm. To explore convergence of individuals, we predefined the number of genetic clusters *K* from 1 to 9. We calculated the *p*-distance matrix using VCF2Dis (https://github.com/BGI-shenzhen/VCF2Dis) and a neighbor-joining tree was generated using the R package APE[66].

Calculation of genetic diversity. Pairwise nucleotide diversity θ_π and Watterson's estimator θ_w[67] within a tiger subspecies were calculated using a sliding-window approach (20-kb windows sliding in 10-kb steps). Genetic differentiation between tiger subspecies was calculated using the pairwise fixation index F_{ST}[68].

Identity-by-state (IBS) and identity-by-descent (IBD) analyses. To evaluate the similarity between two tigers within a subspecies, genome-wide IBS pairwise identities were calculated using the toolset SNPRelate[69] in the R package, based on the matrix of genome-wide IBS pairwise distances, we performed multidimensional scaling analysis and cluster analysis, and determined the groups using a permutation score. We also calculated the pairwise IBD using PLINK (v1.9)[64].

Introgression and demographic history analyses. We separated the South China tigers into three classes (i.e., subgroup 1, subgroup 2, and ptam1) based on phylogeny. TreeMix (v1.13)[70] was used to detect gene flow between the tiger subspecies based on genome-wide allele frequency data at individual SNPs. We first constructed a maximum-likelihood tree for the subspecies using blocks of 10,000 SNPs. The number of migration events was set from 1 to 6. We calculated introgression among the tiger subspecies using Patterson's D-statistic (ABBA-BABA test)[71], with the cat as the outgroup, and tested the proportions of admixture events (*f4*-ratio) within each South China tiger using Dsuite (v0.4)[30].

We used the PSMC[72] model to reconstruct demographic history. To estimate effective ancestral population size changes for individual tiger subspecies, we selected individuals with high sequencing depth to ensure the quality of the consensus sequence. SNPs were detected using SAMtools[61], sites were filtered based on a minimum depth (DP = 4) or high depth (DP = 50) and mapping quality (Q = 20). We only retained autosomal SNPs. Parameters were set to: -N30, -t15, -r5, -p‘4+25*2+4+6’.

MSMC2[73] was used to infer population separation history. To obtain a greater resolution, we estimated divergence times between the two South China tiger subgroups using eight haplotypes per group. We also applied this method to determine divergence between the South China tigers and each of other tiger subspecies using two haplotypes per group.

δaδi[74] analysis was further employed to detect the differentiation time of the two South China tiger subgroups. Only SNPs in intergenic regions were remained to ensure their neutrality. We imputed ungenotyped markers and phased genotypes using BEAGLE[75]. Besides, SNPs with MAF < 0.01 were filtered. The model with the maximum log-likelihood value was considered as the optimal one. A mutation rate of 3.5×10^{-9} per base per generation and generation time of 5 years was used.

Analysis of runs of homozygosity (ROH). Regions of homozygosity were extracted for all chromosomes of all individuals based on SNP information. PLINK (v1.9)[64] was

used to detect ROH via a sliding window approach, with the following parameters: '--homozyg-window-snp 100 --homozyg-window-het 2 --homozyg-window-missing 5 --homozyg-snp 100 --homozyg-kb 100 --homozyg-density 10 --homozyg-gap 100'.

Inbreeding coefficient. We measured individual inbreeding using the genomic inbreeding coefficients F_H[33], which is the fraction of IBD of the two alleles in a diploid individual from a common ancestor. F_H was calculated using PLINK (v1.9)[64]. Alternatively, individual genomic inbreeding coefficients was also measured using F_{ROH}[76], which is an estimate of ROH proportion in an individual genome.

Identification of deleterious mutations. The variants leading to functional changes were regarded as candidates of deleterious mutations. Thus, we only analyzed all potential coding region SNPs. SnpEff (v4.3t)[77] was used for genetic variant annotation and functional effect prediction.

Ethics declarations

All necessary research permits and ethics approvals for this study were granted by Guangzhou Zoo (Project number GZ_20180216).

Data and material availability: Genome assemblies and DNA sequencing data were deposited in the GSA database under Project no. PRJCA006384. The *de novo* genome of the South China tiger was deposited under Accession ID GWHBEIN00000000. The

re-sequencing genomic data of 29 South China tigers and a domestic cat were deposited under Accession ID CRA004909.

References

1 Liu, Y. C. *et al.* Genome-wide evolutionary analysis of natural history and adaptation in the world's tigers. *Curr Biol* **28**, 3840-3849 e3846, doi:10.1016/j.cub.2018.09.019 (2018).

2 Luo, S. J. *et al.* Phylogeography and genetic ancestry of tigers (*Panthera tigris*). *PLoS Biol* **2**, e442, doi:10.1371/journal.pbio.0020442 (2004).

3 Luo, S. J., Liu, Y. C. & Xu, X. Tigers of the world: genomics and conservation. *Annu Rev Anim Biosci* **7**, 521-548, doi:10.1146/annurev-animal-020518-115106 (2019).

4 IUCN. *The IUCN red List of threatened species*. Version 2021-2. https://www.iucnredlist.org (2021).

5 Yin, Y. Z. *Studbook of the South China tiger*. (Chongqing Zoological Garden, China, 2016).

6 Tilson, R., Traylor-Holzer, K. & Jiang, Q. M. The decline and impending extinction of the South China tiger. *Oryx* **31**, 243-252, doi:10.1046/j.1365-3008.1997.d01-123.x (2009).

7 Guo, J. Year of the tiger. *Nature* **449**, 16-18, doi:10.1038/449016a (2007).

8 Zhang, W. *et al.* Sorting out the genetic background of the last surviving South China Tigers. *Journal of Heredity* **110**, 641-650, doi:10.1093/jhered/esz034 (2019).

9 Reed, D. H. & Frankham, R. Correlation between fitness and genetic diversity. *Conserv Biol* **17**, 230-237, doi:10.1046/j.1523-1739.2003.01236.x (2003).

10 Vandewoestijne, S., Schtickzelle, N. & Baguette, M. Positive correlation between genetic diversity and fitness in a large, well-connected metapopulation. *BMC Biol* **6**, 46, doi:10.1186/1741-7007-6-46 (2008).

11 Keller, L. F. & Waller, D. M. Inbreeding effects in wild populations. *Trends in Ecology & Evolution* **17**, 230-241, doi:10.1016/S0169-5347(02)02489-8 (2002).

12 Hedrick, P. W. & Garcia-Dorado, A. Understanding inbreeding depression, purging, and genetic rescue. *Trends Ecol Evol* **31**, 940-952, doi:10.1016/j.tree.2016.09.005 (2016).

13 Armstrong, E. E. *et al.* Recent evolutionary history of tigers highlights contrasting roles of genetic drift and selection. *Mol Biol Evol* **38**, 2366-2379, doi:10.1093/molbev/msab032 (2021).

14 Paszkiewicz, K. & Studholme, D. J. *De novo* assembly of short sequence reads. *Brief Bioinform* **11**, 457-472, doi:10.1093/bib/bbq020 (2010).

15 Eid, J. *et al.* Real-time DNA sequencing from single polymerase molecules. *Science* **323**, 133-138, doi:10.1126/science.1162986 (2009).

16 Schwartz, D. C. *et al.* Ordered restriction maps of Saccharomyces cerevisiae chromosomes constructed by optical mapping. *Science* **262**, 110-114, doi:10.1126/science.8211116 (1993).

17 Lieberman-Aiden, E. *et al.* Comprehensive mapping of long-range interactions reveals folding principles of the human genome. *Science* **326**, 289-293,

485 doi:10.1126/science.1181369 (2009).

486 18 Li, R. *et al.* The sequence and *de novo* assembly of the giant panda genome. *Nature*
487 **463**, 311-317, doi:10.1038/nature08696 (2010).

488 19 Armstrong, E.E., Taylor, R.W., Miller, D.E. et al. Long live the king:
489 chromosome-level assembly of the lion (Panthera leo) using linked-read, Hi-C, and
490 long-read data. *BMC Biol* **18**, doi:10.1186/s12915-019-0734-5 (2020).

491 20 Cho, Y. S. *et al.* The tiger genome and comparative analysis with lion and snow
492 leopard genomes. *Nat Commun* **4**, 2433, doi:10.1038/ncomms3433 (2013).

493 21 Kim, S. et al. Comparison of carnivore, omnivore, and herbivore mammalian
494 genomes with a new leopard assembly. *Genome Biol* **17**, 211,
495 doi:10.1186/s13059-016-1071-4 (2016).

496 22 Figueiro, H. V. *et al.* Genome-wide signatures of complex introgression and
497 adaptive evolution in the big cats. *Sci Adv* **3**, e1700299,
498 doi:10.1126/sciadv.1700299 (2017).

499 23 Simao, F. A., Waterhouse, R. M., Ioannidis, P., Kriventseva, E. V. & Zdobnov, E. M.
500 BUSCO: assessing genome assembly and annotation completeness with
501 single-copy orthologs. *Bioinformatics* **31**, 3210-3212,
502 doi:10.1093/bioinformatics/btv351 (2015).

503 24 Xue, H. R. *et al.* Genetic ancestry of the extinct Javan and Bali tigers. *J Hered* **106**,
504 247-257, doi:10.1093/jhered/esv002 (2015).

505 25 Driscoll, C. A. *et al.* Mitochondrial phylogeography illuminates the origin of the
506 extinct caspian tiger and its relationship to the amur tiger. *PLoS One* **4**, e4125,

507 doi:10.1371/journal.pone.0004125 (2009).
508 26 Foote, A. D. *et al.* Genome-culture coevolution promotes rapid divergence of killer
509 whale ecotypes. *Nat Commun* **7**, 11693, doi:10.1038/ncomms11693 (2016).
510 27 Wang, L. G. *et al*. Genomic analysis reveals specific patterns of homozygosity and
511 heterozygosity in inbred pigs. *Animals* **9**, 314, doi:10.3390/ani9060314 (2019).
512 28 Zeng, L. *et al.* Genomes reveal selective sweeps in kiang and donkey for
513 high-altitude adaptation. *Zool Res* **42**, 450-460,
514 doi:10.24272/j.issn.2095-8137.2021.095 (2021).
515 29 Green, R. E. *et al.* A draft sequence of the Neandertal genome. *Science* **328**,
516 710-722, doi:10.1126/science.1188021 (2010).
517 30 Malinsky, M., Matschiner, M. & Svardal, H. Dsuite - Fast D-statistics and related
518 admixture evidence from VCF files. *Mol Ecol Resour* **21**, 584-595,
519 doi:10.1111/1755-0998.13265 (2021).
520 31 Zeng, L. *et al.* Whole genomes and transcriptomes reveal adaptation and
521 domestication of pistachio. *Genome Biol* **20**, 79, doi:10.1186/s13059-019-1686-3
522 (2019).
523 32 Kardos, M. *et al.* Genomic consequences of intensive inbreeding in an isolated
524 wolf population. *Nat Ecol Evol* **2**, 124-131, doi:10.1038/s41559-017-0375-4
525 (2018).
526 33 Kardos, M., Luikart, G. & Allendorf, F. W. Measuring individual inbreeding in the
527 age of genomics: marker-based measures are better than pedigrees. *Heredity* **115**,
528 63-72, doi:10.1038/hdy.2015.17 (2015).

34 van Oosterhout, C. Mutation load is the spectre of species conservation. *Nat Ecol Evol* **4**, 1004-1006, doi:10.1038/s41559-020-1204-8 (2020).

35 Grossen, C., Guillaume, F., Keller, L. F. & Croll, D. Purging of highly deleterious mutations through severe bottlenecks in Alpine ibex. *Nature Commun* **11**, doi:100110.1038/s41467-020-14803-1 (2020).

36 Feng, S. *et al.* The genomic footprints of the fall and recovery of the Crested Ibis. *Curr Biol* **29**, 340-349 e347, doi:10.1016/j.cub.2018.12.008 (2019).

37 Xue, Y. *et al.* Mountain gorilla genomes reveal the impact of long-term population decline and inbreeding. *Science* **348**, 242-245, doi:10.1126/science.aaa3952 (2015).

38 Li, H. & Durbin, R. Fast and accurate short read alignment with Burrows-Wheeler transform. *Bioinformatics* **25**, 1754-1760, doi:10.1093/bioinformatics/btp324 (2009).

39 Walker, B. J. *et al.* Pilon: an integrated tool for comprehensive microbial variant detection and genome assembly improvement. *PLoS One* **9**, e112963, doi:10.1371/journal.pone.0112963 (2014).

40 Lam, E. T. *et al.* Genome mapping on nanochannel arrays for structural variation analysis and sequence assembly. *Nat Biotechnol* **30**, 771-776, doi:10.1038/nbt.2303 (2012).

41 Langmead, B. & Salzberg, S. L. Fast gapped-read alignment with Bowtie 2. *Nat Methods* **9**, 357-359, doi:10.1038/nmeth.1923 (2012).

42 Servant, N. *et al.* HiC-Pro: an optimized and flexible pipeline for Hi-C data processing. *Genome Biol* **16**, 259, doi:10.1186/s13059-015-0831-x (2015).

551 43 Durand, N. C. *et al.* Juicer provides a one-click system for analyzing
552 loop-resolution Hi-C experiments. *Cell Syst* **3**, 95-98,
553 doi:10.1016/j.cels.2016.07.002 (2016).
554 44 Dudchenko, O. *et al. De novo* assembly of the *Aedes aegypti* genome using Hi-C
555 yields chromosome-length scaffolds. *Science* **356**, 92-95,
556 doi:10.1126/science.aal3327 (2017).
557 45 Robinson, J. T. *et al*. Juicebox.js provides a cloud-based visualization system for
558 Hi-C data. *Cell Syst* **6**, 256-258.e1. doi:10.1016/j.cels.2018.01.001 (2018).
559 46 Tarailo-Graovac, M. & Chen, N. Using RepeatMasker to identify repetitive
560 elements in genomic sequences. *Curr Protoc Bioinformatics* **Chapter 4**, Unit 4.10,
561 doi:10.1002/0471250953.bi0410s25 (2009).
562 47 Bao, W., Kojima, K. K. & Kohany, O. Repbase update, a database of repetitive
563 elements in eukaryotic genomes. *Mob DNA* **6**, 11, doi:10.1186/s13100-015-0041-9
564 (2015).
565 48 Jurka, J. *et al.* Repbase update, a database of eukaryotic repetitive elements.
566 *Cytogenet Genome Res* **110**, 462-467, doi:10.1159/000084979 (2005).
567 49 Gremme, G., Steinbiss, S. & Kurtz, S. GenomeTools: a comprehensive software
568 library for efficient processing of structured genome annotations. *IEEE/ACM Trans*
569 *Comput Biol Bioinform* **10**, 645-656, doi:10.1109/TCBB.2013.68 (2013).
570 50 Benson, G. Tandem repeats finder: a program to analyze DNA sequences. *Nucleic*
571 *Acids Res* **27**, 573-580, doi:10.1093/nar/27.2.573 (1999).
572 51 Altschul, S. F., Gish, W., Miller, W., Myers, E. W. & Lipman, D. J. Basic local

alignment search tool. *J Mol Biol* **215**, 403-410, doi:10.1016/S0022-2836(05)80360-2 (1990).

52 Birney, E., Clamp, M. & Durbin, R. GeneWise and Genomewise. *Genome Res* **14**, 988-995, doi:10.1101/gr.1865504 (2004).

53 Boeckmann, B. *et al.* The SWISS-PROT protein knowledgebase and its supplement TrEMBL in 2003. *Nucleic Acids Res* **31**, 365-370, doi:10.1093/nar/gkg095 (2003).

54 Kanehisa, M. & Goto, S. KEGG: kyoto encyclopedia of genes and genomes. *Nucleic Acids Res* **28**, 27-30, doi:10.1093/nar/28.1.27 (2000).

55 Tatusov, R. L. *et al.* The COG database: an updated version includes eukaryotes. *BMC Bioinformatics* **4**, 41, doi:10.1186/1471-2105-4-41 (2003).

56 Mulder, N. & Apweiler, R. InterPro and InterProScan: tools for protein sequence classification and comparison. *Methods Mol Biol* **396**, 59-70, doi:10.1007/978-1-59745-515-2_5 (2007).

57 Lowe, T. M. & Eddy, S. R. tRNAscan-SE: a program for improved detection of transfer RNA genes in genomic sequence. *Nucleic Acids Res* **25**, 955-964, doi:10.1093/nar/25.5.955 (1997).

58 Griffiths-Jones, S. *et al.* Rfam: annotating non-coding RNAs in complete genomes. *Nucleic Acids Res* **33**, D121-124, doi:10.1093/nar/gki081 (2005).

59 Nawrocki, E. P., Kolbe, D. L. & Eddy, S. R. Infernal 1.0: inference of RNA alignments. *Bioinformatics* **25**, 1335-1337, doi:10.1093/bioinformatics/btp157 (2009).

595 60 Li, H. Aligning sequence reads, clone sequences and assembly contigs with
596 BWA-MEM. **arXiv**, arXiv:1303.3997 (2013).
597 61 Li, H. *et al.* The Sequence Alignment/Map format and SAMtools. *Bioinformatics*
598 **25**, 2078-2079, doi:10.1093/bioinformatics/btp352 (2009).
599 62 McKenna, A. *et al.* The Genome Analysis Toolkit: a MapReduce framework for
600 analyzing next-generation DNA sequencing data. *Genome Res* **20**, 1297-1303,
601 doi:10.1101/gr.107524.110 (2010).
602 63 Wang, K., Li, M. & Hakonarson, H. ANNOVAR: functional annotation of genetic
603 variants from high-throughput sequencing data. *Nucleic Acids Res* **38**, e164,
604 doi:10.1093/nar/gkq603 (2010).
605 64 Purcell, S. *et al.* PLINK: a tool set for whole-genome association and
606 population-based linkage analyses. *Am J Hum Genet* **81**, 559-575,
607 doi:10.1086/519795 (2007).
608 65 Alexander, D. H., Novembre, J. & Lange, K. Fast model-based estimation of
609 ancestry in unrelated individuals. *Genome Res* **19**, 1655-1664,
610 doi:10.1101/gr.094052.109 (2009).
611 66 Paradis, E., Claude, J. & Strimmer, K. APE: Analyses of phylogenetics and
612 evolution in R language. *Bioinformatics* **20**, 289-290,
613 doi:10.1093/bioinformatics/btg412 (2004).
614 67 Nei, M. & Li, W. H. Mathematical model for studying genetic variation in terms of
615 restriction endonucleases. *Proc Natl Acad Sci U S A* **76**, 5269-5273,
616 doi:10.1073/pnas.76.10.5269 (1979).

617 68 Weir, B. S. & Cockerham, C. C. Estimating *F*-statistics for the analysis of
618 population structure. *Evolution* **38**, 1358-1370,
619 doi:10.1111/j.1558-5646.1984.tb05657.x (1984).
620 69 Zheng, X. *et al.* A high-performance computing toolset for relatedness and
621 principal component analysis of SNP data. *Bioinformatics* **28**, 3326-3328,
622 doi:10.1093/bioinformatics/bts606 (2012).
623 70 Pickrell, J. K. & Pritchard, J. K. Inference of population splits and mixtures from
624 genome-wide allele frequency data. *PLoS Genet* **8**, e1002967,
625 doi:10.1371/journal.pgen.1002967 (2012).
626 71 Patterson, N. *et al.* Ancient admixture in human history. *Genetics* **192**, 1065-1093,
627 doi:10.1534/genetics.112.145037 (2012).
628 72 Li, H. & Durbin, R. Inference of human population history from individual
629 whole-genome sequences. *Nature* **475**, 493-496, doi:10.1038/nature10231 (2011).
630 73 Schiffels, S. & Durbin, R. Inferring human population size and separation history
631 from multiple genome sequences. *Nat Genet* **46**, 919-925, doi:10.1038/ng.3015
632 (2014).
633 74 Gutenkunst, R. N., Hernandez, R. D., Williamson, S. H. & Bustamante, C. D.
634 Inferring the joint demographic history of multiple populations from
635 multidimensional SNP frequency data. *PLoS Genet* **5**, e1000695,
636 doi:10.1371/journal.pgen.1000695 (2009).
637 75 Browning, S. R. & Browning, B. L. Rapid and accurate haplotype phasing and
638 missing-data inference for whole-genome association studies by use of localized

haplotype clustering. *American Journal of Human Genetics* **81**, 1084-1097, doi:10.1086/521987 (2007).

76 Kardos, M., Qvarnstrom, A. & Ellegren, H. Inferring individual inbreeding and demographic history from segments of identity by descent in *Ficedula* flycatcher genome sequences. *Genetics* **205**, 1319-1334, doi:10.1534/genetics.116.198861 (2017).

77 Cingolani, P. *et al.* A program for annotating and predicting the effects of single nucleotide polymorphisms, SnpEff: SNPs in the genome of *Drosophila melanogaster* strain w1118; iso-2; iso-3. *Fly (Austin)* **6**, 80-92, doi:10.4161/fly.19695 (2012).

Acknowledgments

We thank Z.J.C., A.P.J., Q.R.W., and X.J.C. from Guangzhou Zoo for providing support during this study. This work was supported by the Science and Technology Program of Guangzhou, China (202102020815).

Author contributions

W.C., X.L.T., C.W., and D.D.W. led the project. C.W., X.L.T., and D.D.W. drafted the manuscript. X.L.T, D.D.W., and M.C.Y. performed data analysis. W.C., Y.H.Y., Y.J.W., M.H., S.M.P., Q.H.C., F.S., J.Y.Y., Q.X.L., Z.Y.L., L.X.L., M.S.T., W.H., J.Y.Z., C.Z., and J.L.H. provided materials. All authors read and approved the final version of the manuscript.

Additional information

Competing interests: The authors declare no competing financial interests.

Figure legends

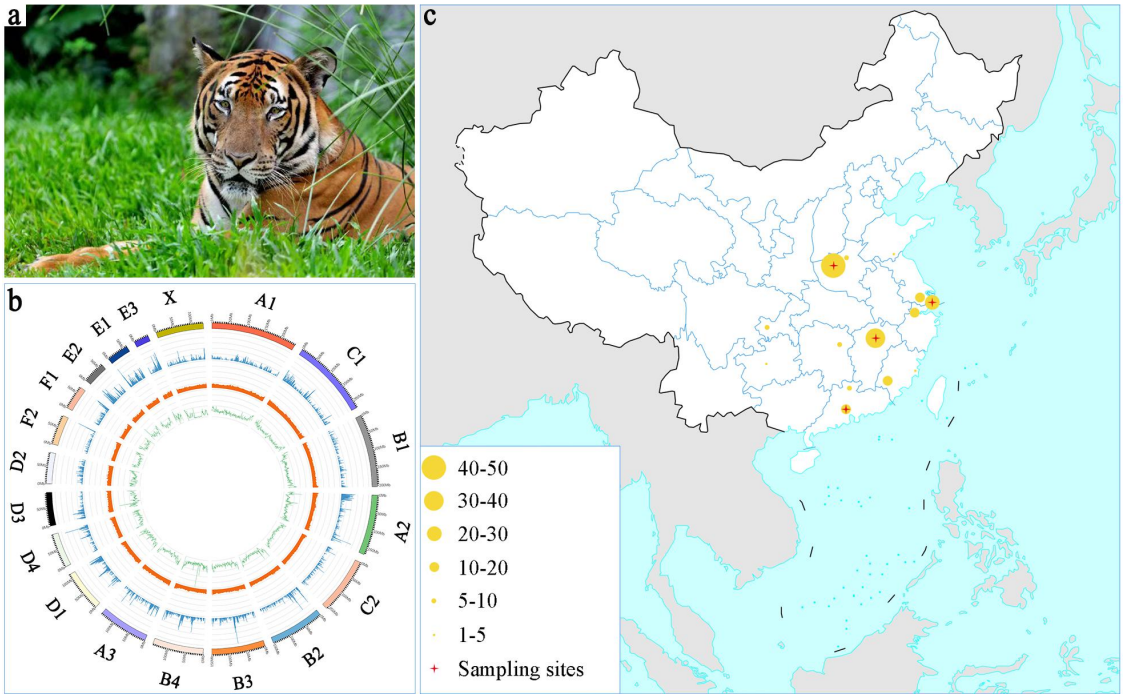

Fig. 1 | Genome of South China tiger. (a) A male South China tiger. (b) Circos plot of South China tiger genomic features. Outer to inner: pseudochromosome, gene density (500-kb window) (with higher gene density indicated by higher blue column), GC content (500-kb window), and SNP density (500-kb window). (c) Distribution of captive South China tigers in China. Yellow circles show 15 city locations of captive South China tigers, including Luoyang, Zhengzhou, Linyi, Suzhou, Shanghai, Hangzhou, Nanchang, Chongqing, Chengdu, Guiyang, Changsha, Fuzhou, Longyan, Shaoguan, and Guangzhou. Circle size is proportional the number of South China tigers in each city. All data are from South China tiger studbook (2020). Red cross represents sampling site of the South China tigers in our study.

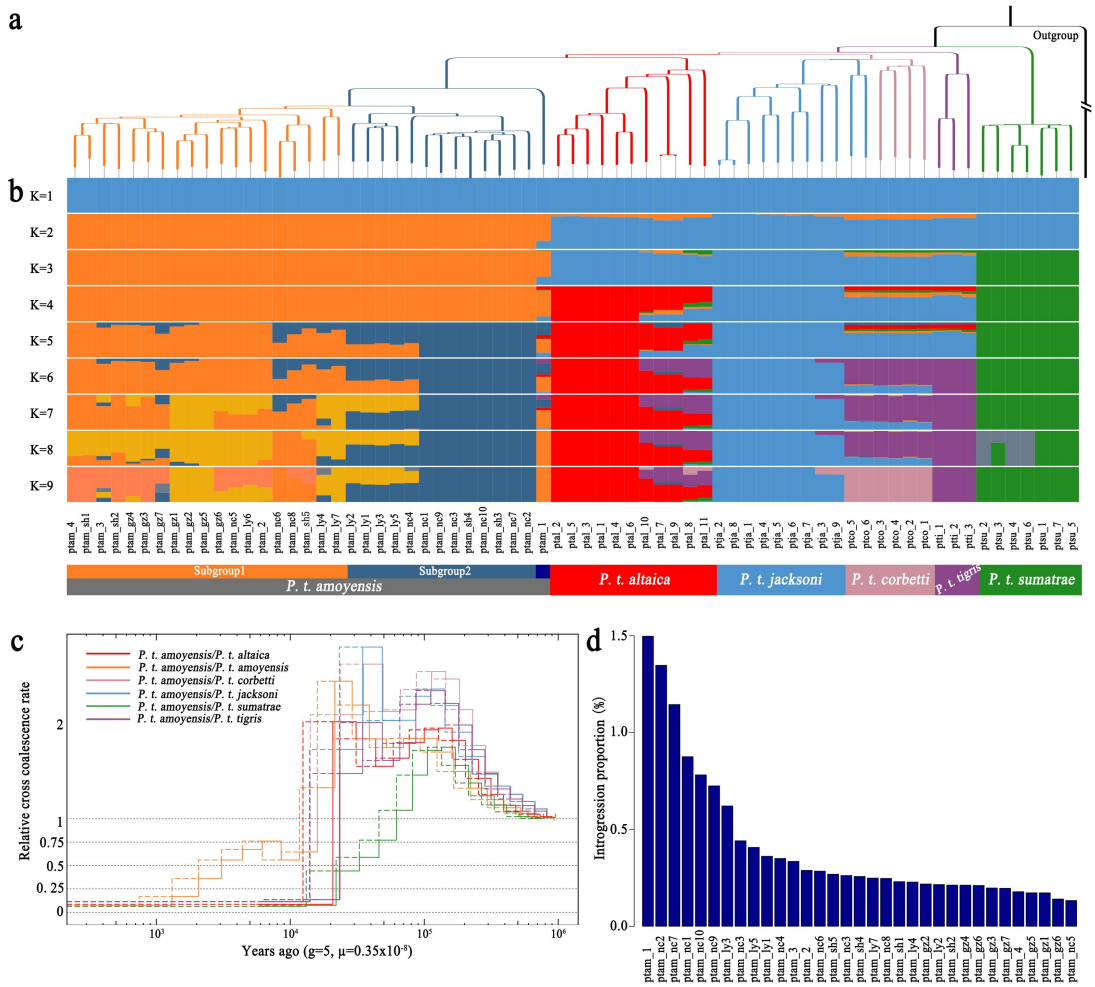

675

676 **Fig. 2 | Genetic components of extant South China tigers.** (a) Phylogenetic relationship of

677 the South China tigers with other tiger subspecies, with a domestic cat as an outgroup. (b)

678 Population genetic structuring of different tiger subspecies. (c) Differentiation time between

679 two sub-populations among the South China tigers (subgroups 1 and 2) and divergence time

680 between the South China tigers and other tiger subspecies inferred by MSMC2. (d) Average

681 ratio of genetic components between the South China tiger and other subspecies.

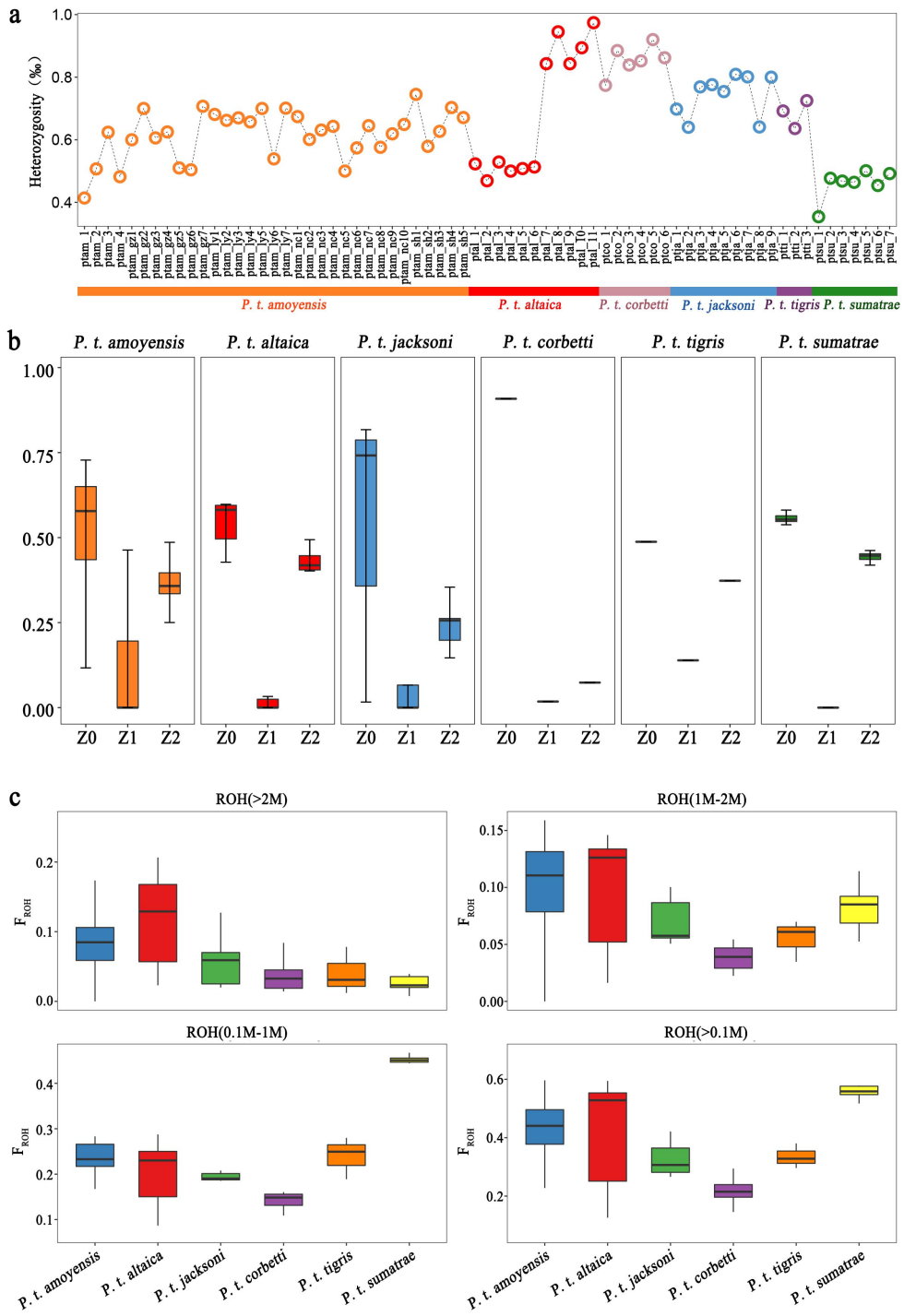

Fig. 3 | Comparison of genetic variation among different tiger subspecies. (a) Genome-wide heterozygosity per individual. (b) Pairwise relatedness based on allelic identity-by-descent (IBD). (c) Genomic inbreeding coefficients (F_{ROH}) based on different lengths of runs of homozygosity (ROH), with a minimum length of 100 kb.

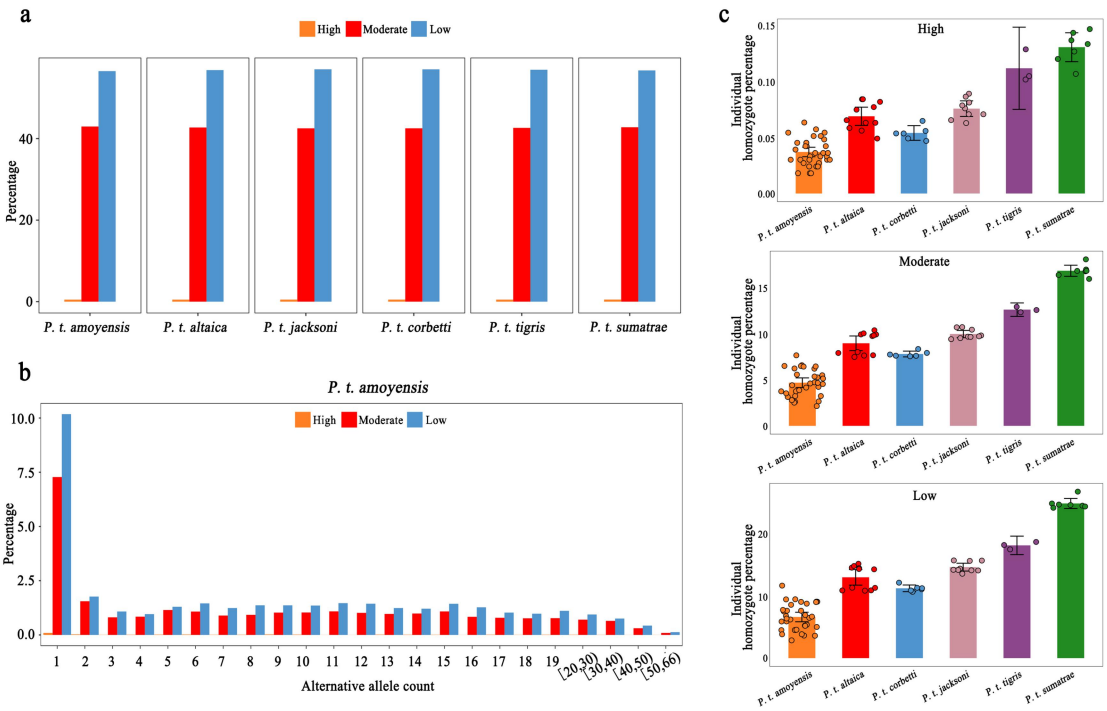

687 **Fig. 4 | Comparison of deleterious mutations among different tiger subspecies.** (a)
688 Percentage of nearly neutral (low), mildly (moderate), and highly deleterious (high impact)
689 mutations in different tiger subspecies. (b) Site frequency spectra for different impact
690 mutations in the South China tigers. Alternative allele counts ≥ 20 are displayed as mean
691 counts per interval. (c) Individual homozygote percentage per impact category and per tiger
692 subspecies.

Supplementary Files

This is a list of supplementary files associated with this preprint. Click to download.

- SupplementTable.pdf
- Supplementarydata.pdf